Experimental evidence of streamwise vortices as finite amplitude solutions in transitional plane Couette flow

S. Bottin, O. Dauchot, and F. Daviaud
Groupe Instabilités et Turbulence, Service de Physique l'État Condensé, Centre d'Études de Saclay, F-91191 Gif-sur-Yvette, France

P. Manneville
Groupe Instabilités et Turbulence, Service de Physique l'État Condensé, Centre d'Études de Saclay, F-91191 Gif-sur-Yvette, France and Laboratoire d'Hydrodynamique, Ecole Polytechnique, F-91128 Palaiseau, France

(Received 16 December 1997; accepted 17 June 1998)

Elongated streamwise structures are considered as a key element of the transition to turbulence in various wall flows. In pure plane Couette flow (pCf), longitudinal streaks originating from pairs of streamwise counter-rotating vortices are clearly identified surrounding growing turbulent spots or at late stages of spot relaxation. The same structures bifurcate subcritically from a slightly modified Couette flow where a thin spanwise wire has been introduced in the zero-velocity plane. The basic flow profile, as measured by laser Doppler velocimetry, is shown to approach continuously the original linear velocity profile as the radius of the wire is decreased. On the other hand, the vortices remain almost unchanged and the bifurcation threshold remains bounded from above by the global stability threshold below which turbulent spots relax spontaneously. This supports the conjecture that a related nontrivial nonlinear solution exists in the pure pCf limit. These observations are compared to numerical stability calculations of the modified flow and to finite amplitude solutions to pCf problems with a different tunable modification. © *1998 American Institute of Physics.* [S1070-6631(98)01010-1]

I. INTRODUCTION

Our understanding of the transition to turbulence in flows of hydrodynamic interest has made important progress during the recent period. This is especially true for systems undergoing supercritical primary bifurcations. Supercriticality is characterized by the fact that the bifurcated state exists only above the linear stability threshold—the critical value of the control parameter, i.e., the Reynolds number R in the present context, beyond which the system is unstable to infinitesimal perturbations—and remains close to the basic state, yielding a continuous transition. This situation can be dealt with using tools of linear and weakly nonlinear stability theory. Rayleigh–Bénard convection is the prototype of supercritical systems. By contrast, regimes emerging from subcritical instabilities are usually much less accessible owing to stronger nonlinear effects. The transition is then discontinuous towards a bifurcated state at a finite distance from the basic state and coexisting with it below threshold. Plane Poiseuille flow is a good example of such systems. It is known to be linearly stable up to Reynolds number $R_l = 5772$[1,2] whereas the branch of two-dimensional nonlinear states emerging from the linearly most unstable modes exists down to $R_{nl} = 2935$.[3] However, "turbulent spots," i.e., fluctuating domains of turbulent flow scattered amidst laminar flow, have been observed down to about $R_c \approx 1000$.[4] Moreover the nature of the perturbations inside the spots bears little connection with the two-dimensional nonlinear states. Plane Couette flow (pCf) is even more extreme since this flow is known to be linearly stable for all values of the Reynolds number,[5,2] which does not preclude a direct transition to turbulence at finite R.[6]

For systems experiencing subcritical bifurcations, one must further distinguish the "natural transition," the threshold of which depends on the noise level, from the "triggered transition" in response to some special perturbation. For natural transition in pCf, early experiments gave a threshold of order $R_c \sim 300$,[7] a more recent one yielding $R_c = 370 \pm 10$.[8] In order to reduce the uncertainty related to the nature of the random fluctuations driving the transition and to investigate the transition more quantitatively, experimentalists have turned to studying the response of the flow to reproducible, well-defined, finite amplitude perturbations. Destabilization of pCf by isolated, instantaneous, localized pulses was then reported for $R_c \approx 360$ in Ref. 9 while other observations in a slightly different experimental configuration gave a somewhat larger value $R_c \approx 370$.[10] In both cases destabilization led to turbulent spots similar to (but also different from) those previously observed in other shear flows (Poiseuille,[4] boundary layer[11]). On the other hand, direct numerical simulations also exhibited sustained turbulent spots for $R > 375$.[12] The origin of the discrepancies between these threshold values was hinted at in Ref. 13 where a critical amplitude of perturbation $A_c(R)$ was shown to exist. This critical amplitude was seen to diverge, or at least to increase sharply, when R was decreased down to $R_{nl} \simeq 325$, the obtained value being consistent with the numerical observation that turbu-

lent pCf cannot be maintained below $R\sim 330$.[14] This issue was further discussed by two of us.[15] In a recent series of experiments[16,17] the value $R_{nl}\simeq 325$ was confirmed as a lower stability limit for the turbulent flow by quenching it down from sufficiently large Reynolds numbers.

Supercritical and subcritical transitions are concepts introduced in classical bifurcation analysis, which appeals for a phase-space approach to the problem in the framework of dynamical systems theory. In this context, understanding a given situation (given control parameters) comes to determining the phase portrait of the system, i.e., the partition of the phase space into basins of attractions associated with the different experimentally observable regimes. Theoretically, it would be desirable to determine directly the different solutions and their stability properties but, except in the simplest cases,[15] this is not possible and one must turn to a more empirical approach by letting the system evolve from a large set of initial conditions. In this sense, detecting the transition by triggering spots can be understood as an *initial value problem*. The result of this study would be a global stability threshold $R_g=\inf R_{nl}$, i.e., the value of the control parameter below which all possible perturbations decay and the flow returns to its basic state asymptotically in time.[18] Another critical value can be analytically determined from the energy method: the threshold for monotonic relaxation R_m below which the kinetic energy contained in any perturbation decays *initially*. For pCf one has $R_m=20.7$,[18] which explains that triggered spots can grow for a while but eventually decay for $R_m<R<R_g$.

Experiments mentioned above suggest $R_g\simeq 325$ for pCf, which is therefore a prototype of *globally subcritical* hydrodynamical systems. The notion of global subcriticality ($R_g<R_l$) was introduced in Ref. 15 in order to clearly distinguish between local weakly nonlinear properties close to the basic state, as given typically by the sign of the first Landau coefficient in an amplitude expansion, and properties for which a global knowledge of the phase space is required, i.e., coexistence of (possibly complicated) attractors each with its own nontrivial basin of attraction. In the latter perspective, the fully nonlinear problem requires a determination of nontrivial solutions, i.e., different from the basic state. The direct search being somewhat uncertain, an indirect approach has been followed by considering a modified system with known solutions and deforming it progressively to recover the original problem. Several numerical studies have tried to capture equilibrium states in pCf by following this *continuous deformation approach*. In this vein, a first possibility was explored by Nagata who considered the circular Couette system between narrow-gap corotating cylinders in the limit of zero average rotation rate, isolating steady solutions in the form of modulated rolls oriented along the flow.[19] Similarly, Clever and Busse investigated a combination of Rayleigh–Bénard convection and simple shear and revealed the existence of subcritical three-dimensional states below the convection threshold, that persisted down to the limit of the pure pCf.[20,21] Both solutions were shown to exist down to $R\sim 125$, a value much lower than the experimental estimate of R_g obtained by the triggering method. This suggests the following alternative: either they have a rather small attraction basin that is difficult to reach from the initial conditions achieved in the experiment, or else (and more probably) they are in fact saddles that are found in the numerics by some limiting process that tracks them along their stable manifold. A different class of solutions was obtained by Cherhabili and Ehrenstein who considered the plane Couette–Poiseuille flow obtained by adding a longitudinal pressure gradient to the basic pCf configuration. Starting from the saturated two-dimensional traveling waves of the classical Poiseuille flow,[3] at the pure pCf limit they obtained nonlinear states in the form of spatially localized two-dimensional stationary states.[22] These solutions were later shown to be unstable against transverse perturbations saturating in three-dimensional localized solutions with smaller structure and at much higher Reynolds numbers $R\sim 1000$,[23] hence possibly less relevant to the structure of the phase space at transitional values of the Reynolds number (~ 300).

Longitudinal roll patterns obtained by the continuous deformation method are good candidates as ingredients of the cyclic process that has been observed in numerical simulations of turbulent pCf: formation of streamwise vortices turning into streaks, breakdown of the streaks into turbulence, and subsequent regeneration of the vortices after damping of the small scale motions.[14,24,25] While this scenario has been illustrated by Waleffe using a model in terms of low-dimensional dynamical systems[26,27] and the mechanism destabilizing the streaks is now better understood,[28] there is still little direct evidence of such unstable equilibrium states. Their trace can be found in several experiments. As a matter of fact, streaky structures have been observed surrounding turbulent spots,[10] and further characterized by velocity measurements.[29] Streamwise turbulent structures periodically organized in the spanwise direction have been shown to exist both in laboratory experiments[30] and in numerical simulations at $R=750$.[31] Finally, in the spirit of the continuous deformation approach, Dauchot and Daviaud showed that the introduction of a thin wire in the central plane, slightly modifying the basic velocity profile, could stabilize streamwise counterrotating vortices localized on both sides of the wire.[32]

The present study first shows how the initial value problem can give some insight into the nature of the nontrivial solutions playing a role in the transition process. It then focuses more on the continuous deformation approach which, while furnishing supplementary proof of their existence, allows a fully quantitative access to them. The experimental setup is described in Sec. II. Section III first illustrates the occurrence of streaks during the decay of a fully turbulent state, and then those appearing upon destabilization of the flow by localized pulses, on the border of sustained spots. Section IV concentrates on the continuous deformation approach and studies the vortices stabilized by the presence of the thin spanwise wire.[32] A quantitative study of the modified basic flow, tentatively compared to available analytical results,[33] shows that the deformation vanishes as the ratio of the wire's diameter to the channel's gap decreases to zero, while the flow nevertheless bifurcates towards the streamwise-streak state. Section V is devoted to a discussion of our results. Comparison is made with recent stability

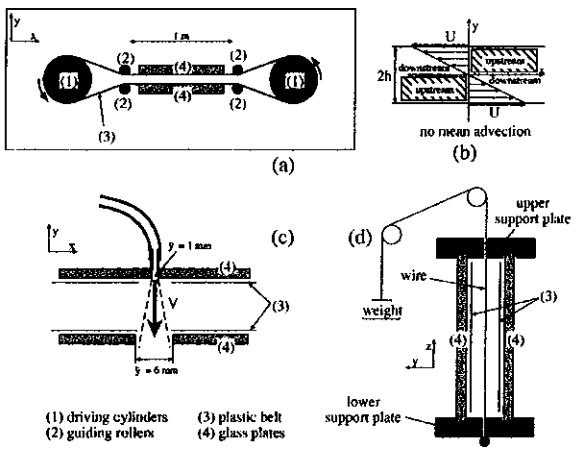

FIG. 1. (a) General view of the plane Couette flow setup. (b) Definition of the shear parameters. When a wire is placed at the origin of coordinates, the four quadrants can be named "upstream" and "downstream" depending on whether the fluid visits the corresponding region before or after having reached the abscissa of the wire. (c) Transverse jet creating the impulse perturbation. (d) Couette flow modified by the wire.

results[34] and with equilibrium states obtained numerically,[19–23] ending with some conclusions about the role of streamwise vortices in transitional pCf.

II. EXPERIMENTAL FACILITIES

The pCf apparatus is sketched in Fig. 1(a):[10] an endless transparent plastic band, the belt, is driven by two large rotating cylinders and guided by two pairs of rollers. The entire apparatus is placed in a tank filled with water, our working fluid. A gap of width d is thus achieved between two "walls" moving in opposite directions and creating a shear flow without mean advection in the fluid, Fig. 1(b). The streamwise direction, the normal to the walls, and the spanwise direction are called x, y, and z, respectively. The test section has a length $L_x \simeq 1$ m. Two different belts with width $L_z = 127$ and 254 mm can be used and the guiding rollers can be adjusted to achieve two gaps, $d = 7$ and 3.5 mm. Table I recapitulates the values of the aspect ratios Γ_x/d and Γ_z/d that have been used.

The Reynolds number is defined as usual by $R = Uh/\nu$ where U is the speed of either wall, $h = d/2$ is the half gap, and ν is the kinematic viscosity of the fluid. U is measured permanently using a nonperturbative optical device with a relative accuracy of ~0.5%. The gap is determined within 0.1 mm with the help of a laser beam focusing device, which makes a relative accuracy of 1.5% or 3% depending on the case. Finally the temperature is controlled within 0.2 K, which induces viscosity variations of less than 5×10^{-8} Stokes, i.e., of order less than 0.5%. The accuracy on R is thus at best 2.5% and at worst 4%.

TABLE I. Experimental aspect ratios $\Gamma_x = L_x/d$ and $\Gamma_z = L_z/d$.

$d = 2h$ (mm)	L_z (mm)	Γ_x	Γ_z
7	127	142	18.1
7	254	142	36.3
3.5	127	286	36.3
3.5	254	286	72.6

Flow visualization and measurements take advantage of the transparency of the belts. A laser sheet produced by a 10 W argon ion laser is used to illuminate the flow, with a CCD camera facing it. The laser sheet can have any orientation, its position being determined within 1 mm. Laminar and turbulent regions can be revealed by seeding the flow with a dilute solution of Merck Iriodin 100 Silver Pearl. This suspension of thin and flat micron-size reflective mica platelets is particularly effective in enhancing the light fluctuations produced by the flow irregularities.[10] This suspension is used for all (x,z) visualizations. A yellow dye can also be introduced at the entrance of the channel, close to the belt, and further advected by the flow down to the center of the experimental domain. This dye is used when observing the vortices in (y,z) planes. Images captured by the camera are recorded on a laser video recorder (LVR) after analog–digital conversion, which allows an image-by-image processing of the movie.

A backscattering laser Doppler velocimetry (LDV) system is used to measure the streamwise velocity U_x. The size of the measurement region is of order 0.075 mm in the x and y direction, so that U_x is averaged over 1% to 2% of the gap. The electronic device controlling the displacement of the probe region has a spatial resolution of order 0.1 mm. The velocity profile $U_x(y)$ and the root-mean-square velocity fluctuation $U_x^{\rm rms}$ are given by a DANTEC burst spectrum analyzer processing the measurement time series. Laminar profiles are determined within an accuracy $U_x^{\rm rms}/U_x$ of order 3%.

The two complementary approaches mentioned in Sec. I, the initial value problem and the continuous deformation method, have been implemented experimentally. In the first approach, triggering of turbulent spots was obtained by means of a brief jet transverse to the pCf, Fig. 1(c). The injection was controlled by an electro-valve and the intensity of the initial perturbation defined as $A = v/U$, where v is the mean velocity of the jet. In the continuous deformation approach, the modified Couette flow was achieved by introducing a thin circular wire of diameter 2ρ parallel to the spanwise direction in the middle of the cell, i.e., $x = z = 0$, Fig. 1(d). Our observations were checked to be independent of the length and the tension of the wire (no detectable effect of the wire's vibrations). The amplitude of the perturbation was set by the ratio of the wire's diameter to the gap $d = 2h$. Table II gives the values of ρ/h used in the experiment.

III. THE INITIAL VALUE PROBLEM

In this section we consider the evolution of the flow from different initial conditions. In a first experiment, the flow is prepared in a sustained turbulent state at large R, typically $R > 500$, and allowed to further evolve as the driving is suddenly decreased to a value less than $R_g = 325$, so that turbulence must decay. Figure 2 displays successive steps separated by 5 s of the flow's relaxation down to R

TABLE II. Values of ρ/h used in the modified Couette flow experiment.

ρ (mm)	0.0125	0.0125	0.032	0.05	0.032	0.05	0.15
h (mm)	3.50	1.75	3.50	3.50	1.75	1.75	3.50
ρ/h	0.0036	0.0071	0.0091	0.0143	0.0182	0.0286	0.0429
ρ (mm)	0.20	0.25	0.15	0.30	0.20	0.25	0.30
h (mm)	3.50	3.50	1.75	3.50	1.75	1.75	1.75
ρ/h	0.0571	0.0714	0.0857	0.0857	0.1143	0.1428	0.1714

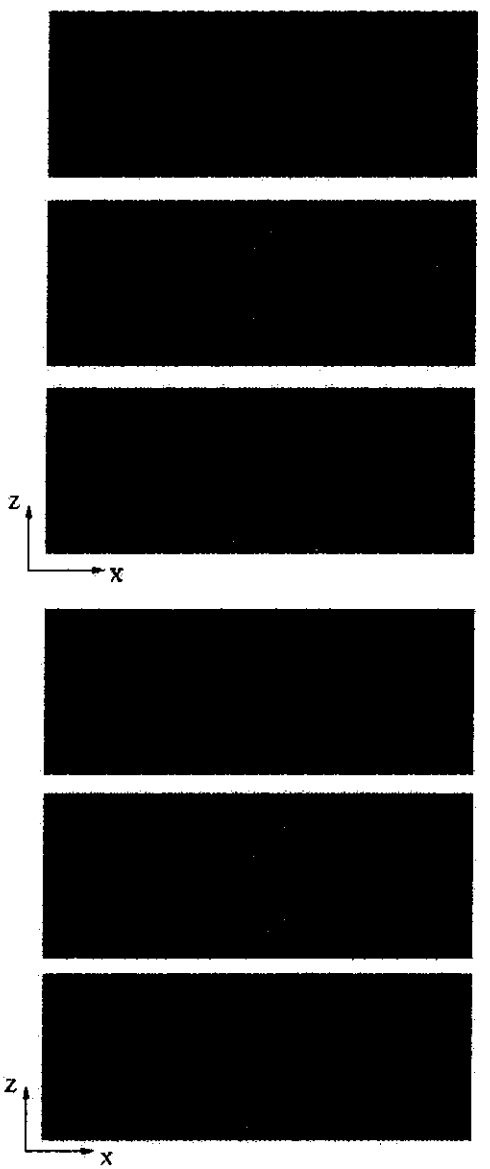

FIG. 2. $(x\text{-}z)$ snapshots of the decay of turbulent plane Couette flow after a sudden slowing down of the imposed shear. (a) From $R>500$ to $R=0$. (b) From $R>500$ to $R=250$.

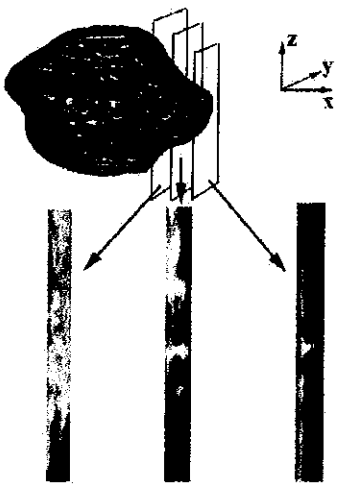

FIG. 3. $(y\text{-}z)$ images of sections of the streamwise counter-rotating vortices at the border of a turbulent spot in successive $(x=\text{const.})$ planes for $R=340$.

$=0$ (a) and 250 (b). A strong difference between the two cases is clearly visible. In case (a) the relaxation process is essentially isotropic in space, which can be understood by noting that all perturbations relax monotonously for $R=0<R_m$, small scales decaying faster than large ones, as expected for processes controlled by viscous dissipation. By contrast, in case (b) the flow goes through anisotropic stages where streamwise streaky structures prevail before the basic laminar pCf is recovered. This can be interpreted by recalling that the final nonlinear decay of solutions occurs along slow manifolds that are the precursors of stable manifolds of states to be observed above R_g.[15] These elongated streamwise streaky structures would therefore be the precursors of actual solutions important for understanding the transition to turbulence under slightly different conditions (higher Reynolds number or/and deformed basic flow).

Let us now turn to another occurrence of similar structures, observed when disturbing pCf by a finite-amplitude local impulse perturbation. Here a short-duration transverse jet flow is used to generate turbulent spots that persist only when the perturbation amplitude A is larger than some critical threshold A_c depending on the Reynolds number. Below $R_g=325$, the flow asymptotically returns to the basic linear velocity profile whatever the intensity of the jet.[13] In pCf, a spot is essentially a quasisymmetrical elliptic patch of turbulent flow, but closer observation reveals a streaky structure in the streamwise direction. Figure 3 displays several sections of the flow at the border of a spot in a $(y\text{-}z)$ plane taken at various distances from its center. The full gap is shown but not the whole spanwise extension L_z (zooming on the relevant part of the picture). Note that the pictures are not taken at the same instant since some time is required for translating the laser plane. The origin of the streaks can be traced back to pairs of streamwise counter-rotating vortices. This is particularly apparent in the first cross view, the most distant from the spot's center. Closer to the center, one can easily

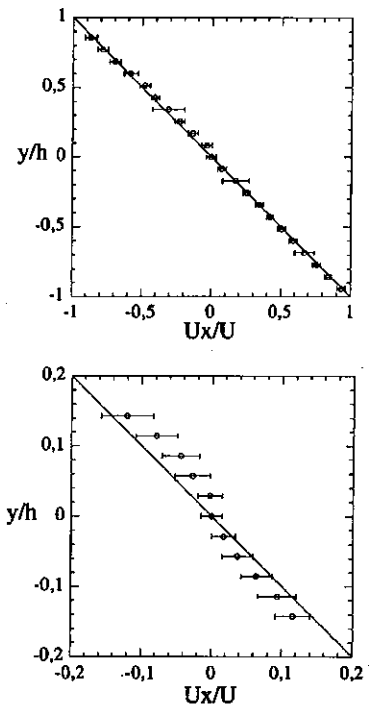

FIG. 4. Streamwise velocity profiles at $x/\rho=1.33$ for $\rho/h=0.043$ and $R=150\pm5$. (a) Whole gap $y/h\in[-1,1]$. (b) Zooming on the central region $y/h\in[-0.15,0.15]$. (The anomalously large error bars are due to the mechanical device used to hold the wire.)

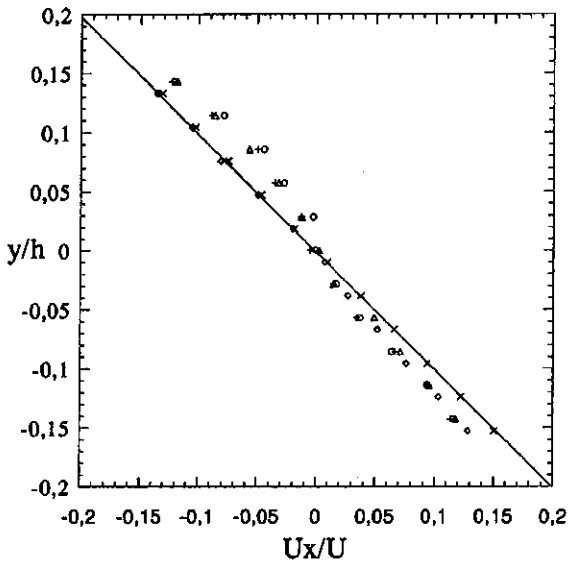

FIG. 5. Velocity profiles at five streamwise locations for $\rho=0.15$ mm, $h=3.5$ mm ($\rho/h=0.043$), and $R=150\pm5$. ○: $x/\rho=-1.33$, +: $x/\rho=-4.00$, △: $x/\rho=-6.66$, ◇: $x/\rho=-9.33$, ×: $x/\rho=-13.33$.

distinguish three regularly spaced vortex pairs and two other pairs ready to form. Even closer to the center, they break down so that it is no longer possible to identify any well-formed structures. Meanwhile mixing is manifestly much stronger.

As already reported in Ref. 13, growing and decaying spots also reveal such streaky structures. When the spot is growing, they develop at its border, regularly spaced, and they propagate in the spanwise direction. When the spot is relaxing, they appear transiently, in much the same way as during the decay of a fully developed turbulent flow (Fig. 2). These transient structures were observed for Reynolds number down to $R=50$, which is much smaller than R_g but larger than R_m. Stronger perturbations are likely to generate the same transient structures for even lower Reynolds number, down to R_m, below which the perturbation energy decays monotonically.

IV. THE CONTINUOUS DEFORMATION APPROACH

The flow is now slightly modified by the introduction of the wire in the zero-velocity plane. Several flow regimes can be distinguished upon increasing R. The featureless basic flow becomes unstable to streamwise vortices that stabilize at a first threshold $R=R_0$. Above another threshold $R=R_2$, the flow is fully turbulent in a band around the wire. In between the detailed transition scenario depends on the value of ρ. We first describe the modified flow, the streamwise vortices, and their breakdown at a given wire radius. Then we study the dependence of our observations on the radius of the wire, focusing on the pure pCf limit $\rho/h\to0$.

A. The modified profile and its destabilization

In this section we mainly consider an experiment with $h=3.5$ mm and a wire of radius $\rho=0.15$ mm ($\rho/h=0.043$).

For $R<R_0=190$, sufficiently close to the wire the flow is different from the classical linear velocity profile, though it remains laminar, stationary, and two dimensional, i.e., translationally invariant in the spanwise direction. Farther from the wire, the linear profile is recovered. The flow can be divided in two domains, an outer one close to the belt, where the flow lines are very slightly disturbed, and an inner one in the center, where the particles turn back.[32] In order to better describe the flow around the wire, the streamwise velocity profile has been measured by LDV at various distances from the wire. As shown in Fig. 4(a), even in the vicinity of the wire ($x=0.2$ mm$=1.33\rho$) and except very close to the central plane, the streamwise velocity profile $U_x(y)$ is only slightly modified. This could be anticipated from the fact that the Reynolds number $R_\rho=U_\rho\rho/\nu=(\rho/h)^2R$, based on the radius ρ of the wire and the unmodified pCf velocity $U_\rho=U\rho/h$ at $y=\rho$, remains very small ($R_\rho<1$) in the R range of interest ($R<400$). Figure 4(b) displays the same profile at a better resolution for $y\simeq0$, confirming that the wire induces a significant but very local deformation of the flow. Compared to the classical linear pCf profile, the streamwise velocity profile now presents an inflection point corresponding to a slowing down close to the central plane.

An estimate of the size of the deformed region can be obtained from Fig. 5 which displays velocity profiles at various streamwise locations ($x<0$). The profiles are no longer

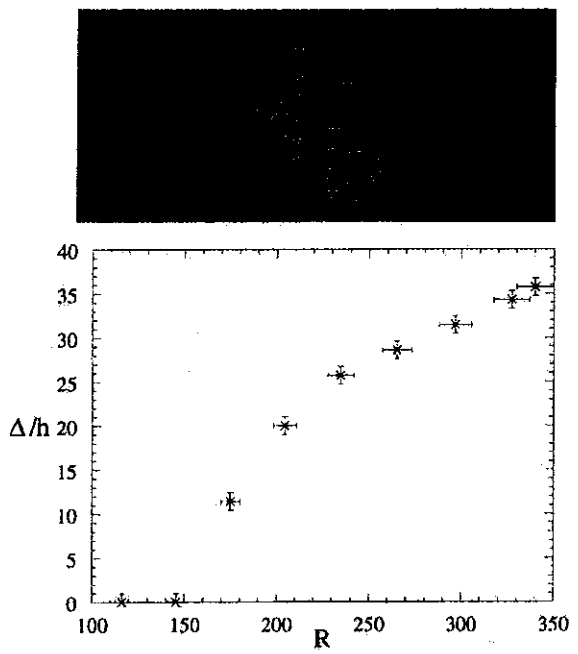

FIG. 6. (a) (x-z) view of the streaks induced by the streamwise vortices for $\rho/h=0.043$ and $R=250$. (b) Δ/h as a function of R for $\rho/h=0.0857$ and $\Gamma_z=36.3$.

symmetric with respect to y. Close to the wire, up to $|x| \sim 1$ mm, the deformation is stronger downstream from the wire ($y>0$) than upstream ($y<0$) [see Fig. 1(b)]. By contrast, farther from the wire, the linear pCf profile is recovered in the downstream region whereas this is not yet the case upstream. We shall return to this observation later (Sec. V).

At $R=R_0$, a transition occurs and coherent structures set in. Regularly spaced along the span, they break the corresponding translational invariance, Fig. 6(a). These coherent structures are easily identified as high velocity streams, usually called *streaks*. These streaks occupy a band of finite width Δ along the wire. Outside this domain, the strength of the vortices is not strong enough to drive the particles and/or the dye from the belt to the central plane, which makes them visually undetectable. Figure 6(b) displays Δ as a function of R. We do not observe qualitative differences when the wire, while remaining in the central plane, is no longer parallel to the spanwise direction but makes an angle θ with the z axis: the vortices remain aligned with the flow and occupy a band parallel to the wire. When measured along the streamwise direction, the width of this band remains the same as in the case $\theta=0$. However, as shown in Fig. 7, R_0 increases rapidly with θ to the point that a wire aligned with the flow ($\theta=\pi/2$) has no apparent destabilizing effect. We consider only $\theta=0$ in the following.

According to previous observations,[32] the origin of the streaks can be attributed to pairs of streamwise counter-rotating vortices. Refined visualizations allow a more complete description of the flow for $R>R_0$. Figure 8 shows sections of the flow in the (y-z) plane close to the wire. Four snapshots separated by 5 s are displayed. As in Fig. 3, a dye

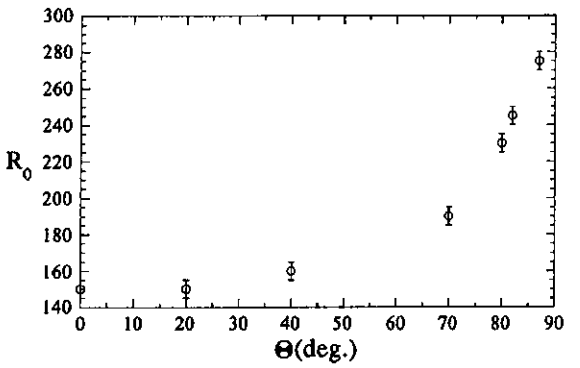

FIG. 7. Dependence of R_0 on the wire tilting angle θ. ($\rho/h=0.0857$, $\Gamma_z=70$.)

is introduced in the flow at $x/h\simeq -250$, and the photograph taken at $x/h\simeq 5$. The typical mushroom shape displayed in the insert is produced by the two counter-rotating vortices (a) and (b) which advect the fluid between them to form the streak(s) according to the well-known *lift-up* mechanism. The vortices appear to be centered in the gap and to have an elliptical section with a long axis d_1 about twice the short one d_2. The ellipses are slightly tilted with respect to the z axis, with opposite tilts for the two vortices in the same pair.

Figure 9 sketches some path-lines that can be inferred from a careful observation of particles floating in the fluid.

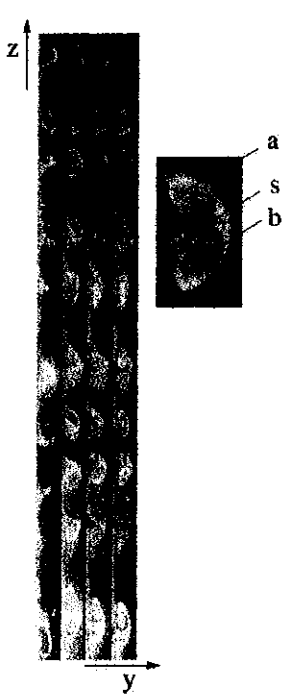

FIG. 8. (y-z) view of the streamwise counter-rotating vortices. Four snapshots at a regular interval of 5 s are displayed. Each image shows the whole gap. The insert displays one given structure made of two vortices (a) and (b) inducing the streak (s) between them by the lift-up mechanism. ($\rho/h=0.0571$, $R=190$.)

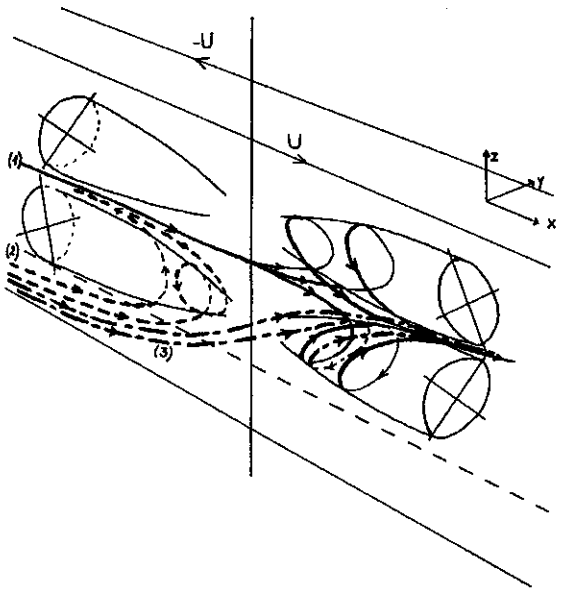

FIG. 9. Schematic view of the streamwise counter-rotating vortices and the trajectories they induced in the shear flow. See text for details.

For the sake of clarity only one pair of vortices is represented on each side of the wire, and only the simplest trajectories coming from one side of the wire are presented, but much more complicated ones also exist. For example, the trajectories represented by a solid line, labeled (1), originate midway between the axes of the two vortices in a given pair. They remain close to the belt until they reach the abscissa of the wire. The direction of rotation of the vortices is then reversed and the trajectories are forced towards the central plane due to the lift-up from which the streaks originate. Trajectories in dashed and dot-dashed lines [labeled (2) and (3)] both originate outside the vortex pair. Two cases can then be distinguished according to whether or not the particles cross the central plane before reaching the abscissa of the wire: if so, the trajectory (dashed) coils around the vortex ahead of the wire after the particle has turned back; if not, the trajectory (dot-dashed) coils around the vortex behind the wire.

The mushroom structures are more or less regularly spaced along the wire. An average periodicity $\Lambda = L_z/\langle N \rangle$ can be measured by counting the mean number of streaks $\langle N \rangle$. To determine it a video sequence of 1200 frames was divided in 30 individual sequences of 40 frames. Each short sequence was played in loop in order to locate the streaks. $\langle N \rangle$ was further obtained by averaging over the 30 individual sequences, yielding $\Lambda/h = 5 \pm 10\%$. No influence of Γ_x and Γ_z could be detected.

In addition to this statistical characterization, we have also examined the local instantaneous structure of the flow. Figure 10(a) displays a typical (y-z) section of the streak pattern. From the position of the streaks indicated by thin vertical bars, it appears that the local spacing λ between two streaks fluctuates somewhat. This observation has been made more precise in Fig. 10(b) where the light intensity profile recorded along the white line in Fig. 10(a) is displayed. From this profile we can distinguish regions in the flow dominated by the vortices (white) from regions of relative inactivity (grey). Whereas the former have a roughly constant width, the size of the latter shows large variations that explain the fluctuations of λ.

Next, upon increasing R the following sequence is observed. The fluctuations of λ become larger and, for R large enough, regions of relative inactivity (grey) may become sufficiently wide to allow the creation of additional vortex pairs. This regime precedes the onset of a second transition at $R = R_1 = 310$ (for $\rho/h = 0.043$), where the streamwise vortices are destabilized by localized intermittent turbulent bursts that nucleate at some point along the wire, fluctuate for a while, and decay to reappear somewhere else. The entire process is strongly reminiscent of spatiotemporal intermittency (STI) observed in some quasi-one-dimensional hydrodynamics experiments[35] and interpreted within the framework of critical phenomena in statistical physics.[36,37] The duration and spatial extent of these bursts increases with R, ending at $R_2 \simeq 325$ in a fully turbulent band along the wire, the streamwise extension of which then grows linearly with the Reynolds number.[32] Now, decreasing R from above R_2, the band of turbulence remains sustained down to $R_3 \simeq R_2$. This scenario holds for $\rho/h = 0.043$ and more generally for ρ/h large enough. A slightly different picture is obtained when ρ/h gets smaller, which suggests studying the limit where the pure pCf is recovered.[38]

B. The modified pCf in the limit $\rho/h \to 0$

We now study the dependence of our observations on the diameter of the wire, summarized in the bifurcation diagram of Fig. 11. Consider first the behavior of R_0. It is readily seen that when $\rho/h \to 0$ the threshold of the bifurcation toward the streak state seemingly extrapolates to some finite value of the order of R_g as determined from the initial value problem for jet perturbations.

When ρ/h is decreased, the basic state from which the flow bifurcates is less and less deformed and the linear velocity profile is recovered closer and closer to the wire as

FIG. 10. (a) (y-z) view of the streamwise counter-rotating vortices with location of the streaks. (b) Intensity prolile taken in (a) along the line. (c) Interpretation: (white)→regions of vortex-dominated dynamics; (grey) →regions of relative inactivity. ($\rho/h = 0.0571$, $R = 190$.)

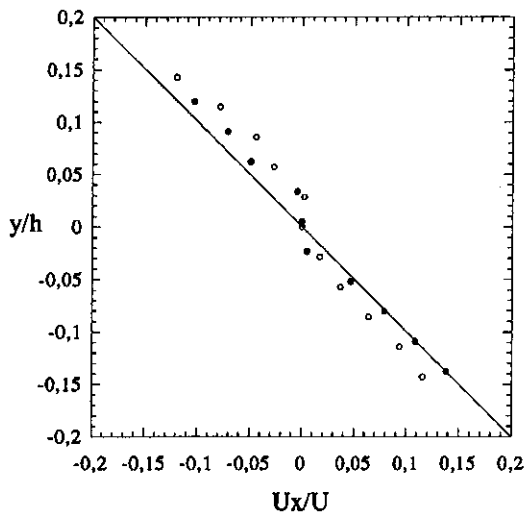

FIG. 11. Bifurcation diagram giving the different thresholds as functions of ρ/h for $\Gamma_z=70$. R_0: transition from the basic state to the streaks; R_1: spatiotemporally intermittent destabilization of the streaks for $\rho/h>0.0186$; R_2 transition to the fully turbulent band; R_3: decay of turbulence into streaks for $\rho/h<0.0186$ when decreasing R. Lines are just given as guides for the eye.

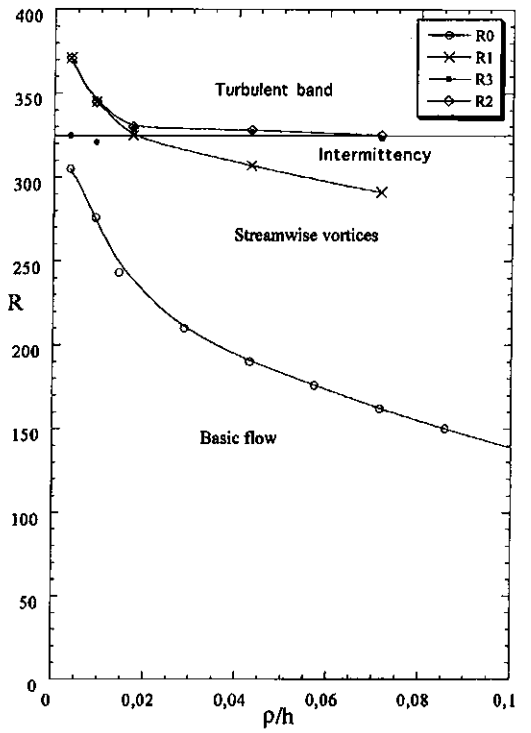

FIG. 12. Streamwise velocity profile at $x/\rho=1.33$. ♦: $\rho/h=0.0143$, ○: $\rho/h=0.043$. ($R=150\pm5$.)

illustrated in Fig. 12 which displays the basic velocity profiles near the central plane at given $x/\rho=1.33$ for two wires of different diameters and $R<R_0$. This does not preclude the streaks from being relatively insensitive to the value of ρ/h. As shown in Fig. 13(a), Λ decreases very slightly and roughly linearly with ρ/h, so that assuming a regular behavior at the pure pCf limit yields $\Lambda\to 4h$. The typical size d_1 of the vortices follows a similar behavior and by extrapolation we get $d_1\to 0.6h$, Fig. 13(b).

These statistical characterizations do not give a qualitative picture of the bifurcated flow at small ρ/h. Figure 14 displays a $(y\text{-}z)$ section of the streamwise counter-rotating vortices for $\rho/h=0.014$, to be compared to that for $\rho/h=0.043$ in Fig. 8. One notices immediately that, though regions of vortex-dominated dynamics and regions of relative inactivity can still be defined, the vortex pairs are not as regularly spaced as they are for the wire with a larger diameter. Furthermore, the description of the flow in terms of a more or less regular cellular pattern is now replaced by an image in terms of domains of different kinds ("active" streak state and "inactive" basic state) separated by fronts. We shall return to this point later.

To conclude this section, let us complete the description of the bifurcation diagram in Fig. 11 and consider the scenario that develops for wires with diameters smaller than $\rho/h\simeq 0.0182$. Instead of the regime of spatiotemporal intermittency described above, the flow now experiences a direct transition from the streak state to turbulence when R is increased ($R_1\simeq R_2$), while the turbulent state can be maintained down to $R_3\simeq 325$ when R is decreased. A striking feature of this bifurcation diagram is that sustained turbulence can be observed throughout the ρ/h range above $R=R_3\simeq 325$ which is precisely the minimal value beyond which turbulent spots can be generated in pure pCf.

V. DISCUSSION

We now address the issues raised by the results presented in previous sections. Since we are mostly interested in the transition to turbulence in pCf, we organize the discussion by first considering the bifurcations of the configuration at large ρ/h for increasing values of R, and next the effect of decreasing the perturbation.

Below the threshold R_0 for steady streamwise vortices, the measured profile exhibits two essential characteristics: (1) a sharp localization of the modification close to the wire, not only in the streamwise direction x but also in the cross-stream direction y, and (2) a clear lack of y-reflection symmetry at any given streamwise location. Theoretical results about the basic flow are scarce. To our knowledge, the only possibly relevant analytical solution, due to Chwang and Wu,[33] concerns the Stokes problem for a wire in an unbounded shear. The corresponding result shows neither the localization (smooth monotonic $1/r$-decay of the velocity corrections to the linear profile) nor the observed lack of symmetry since at given x, it satisfies $U_x(x,-y)=-U_x(x,y)$ and $U_y(x,-y)=U_y(x,y)$. The latter discrepancy is clearly due to the limitations of the Stokes approximation since it is easily checked that this symmetry is not compatible with the nonlinear advection term of the full Navier–Stokes (NS) equations; for example $U_x\partial_x U_x+U_y\partial_y U_x$ does not change sign in the transformation $x\mapsto x$,

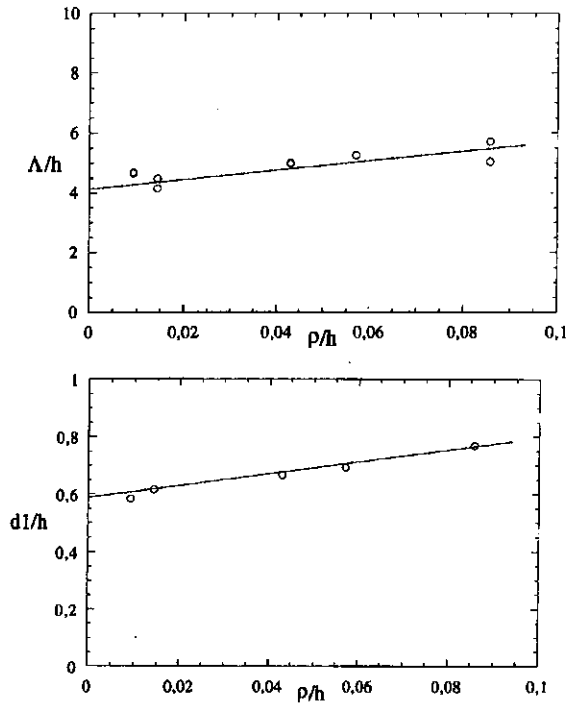

FIG. 13. Average spanwise periodicity Λ/h (a) and mean vortex largest radius $\langle d_l \rangle$ (b) as functions of the reduced wire radius ρ/h. ($\Gamma_z = 70$.)

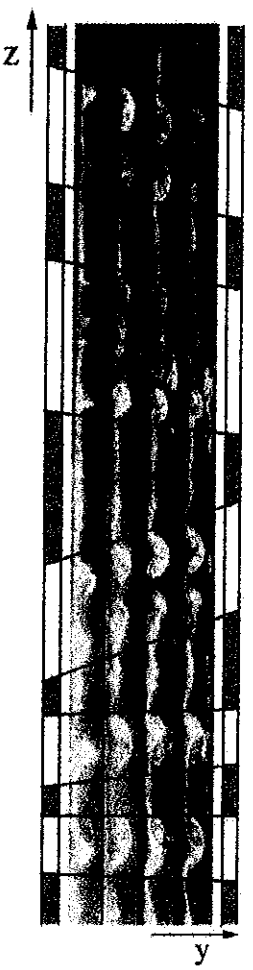

FIG. 14. Four $(y\text{-}z)$ successive snapshots of the streamwise counter-rotating vortices. $\rho/h = 0.0143$, $R = 250$. Each image shows the whole gap. Fronts between areas of vortex-dominated dynamics and areas of relative inactivity are marked by a line.

$y \mapsto -y$. An attempt to go beyond this limitation within the Oseen approximation, still in the unbounded case, is in progress.[39] Recently, motivated by our results, Barkley and Tuckerman[34] studied a configuration similar to ours numerically. In their problem, the wire was replaced by a ribbon of cross-channel width 2ρ for easier numerical implementation, but it was placed at the center of the flow, perpendicularly to the flow direction so that the obstacle had the same apparent section. Seeking steady two-dimensional solutions of the full NS equations they found a solution slightly lacking y-reflection symmetry, though remaining centrosymmetric, i.e., such that $U_x(-x,-y) = -U_x(x,y)$ and $U_y(-x,-y) = -U_y(x,y)$, as expected from the nonlinear terms in the equations. In fact the symmetry breaking obtained in the case of the ribbon seems smaller than that observed around the wire, which is as yet unexplained but probably related to the specific shape of the obstacle. More importantly, the numerical solution shows two distinct regions, one close to the ribbon where the correction to the linear velocity profile corresponds to a circulation opposing the flow (contracirculation), the other farther from the wire where the correction is much weaker and in the same sense (cocirculation). The stagnation point separating the two regions is located at about $x/h = 2.5$ and does not depend much on the ratio ρ/h (two values $\rho/h = 0.086$ and 0.043 have been considered). These findings are in agreement with the observed fact that the flow seems to return quite abruptly to the linear profile at some distance from the wire (Fig. 5). A fully quantitative comparison is not possible owing to both the difficulty in obtaining experimental velocity profiles and the difference in the obstacle's shape.

For $R_0 \leqslant R \leqslant R_1$, a wide band of streamwise streaks along the wire is experimentally observed. The streamwise extension Δ of these streaks is much larger than the region where the profile is significantly modified by the the presence of the wire. This immediately leads one to think that the flow has switched to a new state that has little to do with the modified basic state. Accordingly, this new state can be seen as resulting not from the saturation of a linear instability mode but rather as a fully nonlinear state. This idea is further supported by the light intensity profile displayed in Fig. 10. Indeed, the alternation of regions of low and high intensity, separated by sharp edges, implies the presence of a large amount of high harmonics typical of a strongly nonlinear solution, not what one would expect from the weakly nonlinear saturation of the amplitude of a linear mode. In contrast this fits more with what would result from a subcritical

instability where the bifurcated state stays at a finite distance from the basic state so that the solution may be composed of domains of either state separated by fronts. The observation that, during the very first steps of the transition process, some streaks first develop in limited domains and next contaminate the whole span further supports this idea.

While direct experimental evidence of subcriticality *via* the determination of hysteresis has not yet been obtained, subcriticality was unambiguously detected in the numerical approach of Barkley and Tuckerman[34] who determined the linear instability threshold of the modified basic flow and further studied the development of the three-dimensional primary mode they obtained. A thorough comparison of experimental and numerical findings is not possible for the moment since, as explained above, the experiment gives us at best an estimate of the nonlinear threshold while, up to now, the numerics only predicts the linear threshold but has not yet been extended to yield the nonlinear threshold. However, our results are clearly compatible: First the values obtained numerically fall in the same range ($R_1=230$ and 550 for $\rho/h=0.086$ and 0.043, respectively) and are somewhat larger than the corresponding experimental values of R_0 (Fig. 11). Second, the critical wavelength is numerically seen to depend little on ρ/h. Values found for $\rho/h=0.086$ and 0.043 are $\lambda_c=4.87h$ and $4.48h$, in good agreement with the experimental values shown in Fig. 13. Finally, the structure of the nonlinear saturated state is also somewhat different from that of the critical linear eigenmode, especially regarding the streamwise shape of the perturbation, which suggests that a width Δ can be defined for the region occupied by the streamwise vortices. Furthermore this width is much larger than the width of the region where the amplitude of the critical mode is significant, which is also in agreement with the experiments showing that Δ is much larger than the zone where the basic flow is deformed.

The rapid increase of R_1 as ρ/h is divided by two is consistent with a divergence as ρ/h tends to zero. By contrast, as seen in Fig. 11 in the experiments, R_0 seems to extrapolate to a finite value of the order of 325. This fact requires some explanation since at the limit $\rho\to 0$ one expects to recover the linearly stable pCf. From this, one should infer that R_0 increases without bound as ρ decreases only if one was sure to detect a linear instability threshold comparable to that obtained in Ref. 34. However, it is more likely that the instability converts from supercritical at large ρ/h to more and more subcritical as ρ/h tends to zero. In this perspective, R_0 would correspond rather to an effective nonlinear instability threshold detected from the development of a structure excited by residual turbulence, and thus already out of the attraction basin of the unmodified Couette flow. Limitations of the present setup forbid us to say more but, in this context, transition observed experimentally for $\rho/h\leqslant 0.014$ is particularly interesting: the observed flow pattern seems to be composed of coexisting domains of strong vorticity and relative inactivity that are reminiscent of the picture given by Pomeau[36] for a subcritical system where two states are in competition. Active regions where the streamwise vortices are conspicuous should be portions of nonlinear solutions belonging to a branch disconnected from the basic unmodified pCf solution that would be relevant to inactive regions. The streamwise localization is easily understood from the fact that, at sufficient distance from the wire, the flow has, at any rate, returned to a linear velocity profile that is the only possible steady solution for $R<325$. In turn, this also explains the hysteretic behavior observed around the thinnest wires: by starting an experiment with $325<R_2<R$, which triggers the streamwise vortices, and then decreasing R the turbulent solution is retained down to $R_3\simeq 325$.

These considerations suggest that we can overlook the specific origin of the streamwise vortices and relate them to the numerical solutions obtained by Busse and Clever,[21] Nagata,[19] and Cherhabili and Ehrenstein.[22] These solutions were found by various continuation methods similar to our continuous deformation approach. They were obtained as essentially unstable three-dimensional steady states of the full NS equations. All of these solutions display strong qualitative differences with our streamwise vortices. Solutions reported in Refs. 21 and 19, though at Reynolds numbers in the correct range, are periodic in the streamwise direction and remain unlocalized. Solutions obtained in Ref. 23 are indeed localized along x but the spanwise periodicity and the order of magnitude of the Reynolds numbers strongly disagree. By contrast, one can conjecture that the slowly varying background provided by the localized modification to the basic flow, as achieved in the present experiment as well as the numerical simulations of Barkley and Tuckerman,[34] is able to stabilize pre-existent nonlinear solutions that could not be observed otherwise. The occurrence of streamwise vortices observed in Fig. 3 at the edge of a sustained turbulent spot might also be another consequence of this process since turbulence within the spot is expected to modify the mean flow.

To conclude, we have taken advantage of the subcritical character of the plane Couette flow to stabilize localized streamwise vortices. We have related these vortices to the existence of nonlinear solutions that are only unstable and transient in a natural environment. The results of this study, which concentrates on one of the steps of the cyclic process of regeneration and breakdown at work in turbulent shear flows, thus seem of more general interest in the context of transitional wall-bounded flows.

[1]S. A. Orszag, "Accurate solution of the Orr–Sommerfeld stability equation," J. Fluid Mech. **50**, 689 (1971).
[2]P. G. Drazin and W. H. Reid, *Hydrodynamic stability* (Cambridge University Press, Cambridge, England, 1981).
[3]T. Herbert, "Periodic secondary motions in a plane channel flow," in *Proceedings of International Conference on Numerical Methods in Fluid Dynamics*, edited by A. I. van de Vooren and P. J. Zandbergen (Springer-Verlag, Berlin, 1976), p. 235.
[4]D. R. Carlson, S. E. Widnall, and M. F. Peters, "A flow-visualization study of transition in plane Poiseuille flow," J. Fluid Mech. **121**, 487 (1982).
[5]V. A. Romanov, "Stability of plane parallel Couette flow," Funkt. Anal. Ego Priloz. **7**, 62 (1970).
[6]H. Reichardt, "Über die Geschwindigkeitsverteilung in einer geradlinigen turbulenten Couetteströmung," Z. Angew. Math. Mech. **36**, 26 (1956).
[7]H. J. Leutheusser and V. H. Chu, "Experiments on plane Couette flow," J. Hydraul. Div. ASCE **97**, 1269 (1971); M. Aydin and H. J. Leutheusser, "Novel experimental facility for the study of plane Couette flow," Rev. Sci. Instrum. **50**, 1362 (1979).
[8]S. Malerud, K. J. Måløy, and W. I. Goldburg, "Measurements of turbulent

velocity fluctuations in a planar Couette cell," Phys. Fluids **7**, 1949 (1995).
[9]N. Tillmark and P. H. Alfredsson, "Experiments on transition in plane Couette flow," J. Fluid Mech. **235**, 89 (1992).
[10]F. Daviaud, J. Hegseth, and P. Bergé, "Subcritical transition to turbulence in plane Couette flow," Phys. Rev. Lett. **69**, 2511 (1992).
[11]H. W. Emmons and A. E. Bryson, "The laminar-turbulent transition in a boundary layer," J.A.S. **18**, 490 (1951).
[12]A. Lundbladh and A. Johansson, "Direct simulation of turbulent spots in plane Couette flow," J. Fluid Mech. **229**, 499 (1991).
[13]O. Dauchot and F. Daviaud, "Finite-amplitude perturbation and spots growth mechanism in plane Couette flow," Phys. Fluids **7**, 335 (1995).
[14]J. M. Hamilton, J. Kim, and F. Waleffe, "Regeneration mechanisms of near-wall turbulence structures," J. Fluid Mech. **287**, 317 (1995).
[15]O. Dauchot and P. Manneville, "Local versus global concepts in hydrodynamics stability theory," J. Phys. II **7**, 371 (1997).
[16]S. Bottin, P. Manneville, F. Daviaud, and O. Dauchot, "Discontinuous transition to spa-tiotemporal intermittency in plane Couette flow," to appear in Europhys. Lett.
[17]S. Bottin and H. Chaté, "Statistical analysis of the transition to trubulence in plane Couette flow," to appear in EPJH.
[18]D. D. Joseph, *Stability of Fluid Motions, I.* (Springer-Verlag, Berlin, 1976).
[19]M. Nagata, "Three-dimensional finite-amplitude solutions in plane Couette flow: bifurcation from infinity," J. Fluid Mech. **217**, 519 (1990).
[20]R. M. Clever and F. H. Busse, "Three dimensional convection in a horizontal fluid layer subjected to a constant shear," J. Fluid Mech. **234**, 511 (1992).
[21]F. H. Busse and R. M. Clever, "Bifurcation sequences in problems of thermal convection and of plane Couette flow," in *Waves and Nonlinear Processes in Hydrodynamics*, edited by J. Grue, B. Gjevik, and J. E. Weber (Kluwer, Dordrech, 1996).
[22]A. Cherhabili and U. Ehrenstein, "Spatially localized two-dimensional finite amplitude states in plane Couette flow," Eur. J. Mech. B/Fluids **14**, 677 (1995).
[23]A. Cherhabili and U. Ehrenstein, "Finite-amplitude equilibrium states in plane Couette flow," J. Fluid Mech. **342**, 159 (1997).
[24]F. Waleffe, J. Kim, and J. Hamilton, "On the origin of streaks in turbulent shear flows," in *Turbulent Shear Flows 8* (Springer, New York, 1993).
[25]K. Coughlin, "Coherent structures and intermittent turbulence in channel flows: Part I: Coherent Structures," J. Fluid Mech. (submitted).
[26]F. Waleffe, "Hydrodynamics stability of turbulence: Beyond transients to a self-sustaining process," Stud. Appl. Math. **95**, 319 (1995).
[27]F. Waleffe, "On a self-sustaining process in shear flows," Phys. Fluids **9**, 883 (1997).
[28]S. C. Reddy, P. J. Schmid, J. S. Baggett, and D. S. Henningson, "On stability of streamwise streaks and transition to turbulence in plane channel flows," J. Fluid Mech. **365**, 269 (1998).
[29]N. Tillmark, "On the spreading mechanisms of a turbulent spot in plane Couette flow," Europhys. Lett. **32**, 481 (1995).
[30]K. H. Bech, N. Tillmark, P. H. Alfredsson, and H. I. Andersson, "An investigation of turbulent plane Couette flow at low Reynolds numbers," J. Fluid Mech. **286**, 291 (1995).
[31]J. Komminaho, A. Lundbladh, and A. Johansson, "Very large structures in plane turbulent Couette flow," J. Fluid Mech. **320**, 259 (1996).
[32]O. Dauchot and F. Daviaud, "Streamwise vortices in plane Couette flow," Phys. Fluids **7**, 901 (1995).
[33]A. T. Chwang and T. Wu, "Hydromechanics of low Reynolds-number flow. Part 2. Singularity method for Stokes flows," J. Fluid Mech. **67**, 787 (1975).
[34]D. Barkley and L. S. Tuckerman, "Stability analysis of perturbed plane Couette flow," submitted to Phys. Fluids; first presented at 10th International Couette-Taylor Workshop, Paris, 1997 (laurette@limsi.fr).
[35]F. Daviaud, "Experiments in 1D turbulence," in *Turbulence: A Tentative Dictionary*, edited by P. Tabeling and O. Cardoso (Plenum, New York, 1994).
[36]Y. Pomeau, "Front motion, metastability, and subcritical bifurcations in hydrodynamics," Physica D **23**, 546 (1986).
[37]H. Chaté and P. Manneville, "Spatiotemporal intermittency," in *Turbulence: A Tentative Dictionary*, edited by P. Tabeling and O. Cardoso (Plenum, New York, 1994).
[38]S. Bottin, O. Dauchot, and F. Daviaud, "Intermittency in a locally forced plane Couette flow," Phys. Rev. Lett. **79**, 4377 (1991).
[39]C. Vasilescu and P. Manneville (in preparation).